Vanadium Insertion into CO_2, CS_2 and OCS: A Comparative Theoretical Study

Imre Pápai*

Institute of Isotope and Surface Chemistry, Spectroscopy Department, Chemical Research Centre, HAS H-1525 Budapest, P.O.B. 77, Hungary

Yacine Hannachi, Sylvain Gwizdala, and Joëlle Mascetti

Laboratoire de Physico-Chimie Moléculaire, (UMR 5803 CNRS), Université Bordeaux I, 351, cours de la Libération, 33405 Talence Cedex, France

Received: November 1, 2001; In Final Form: February 14, 2002

The reactions of the ground-state V(s^2d^3) atom with CO_2, CS_2, and OCS molecules have been studied at the B3LYP level of density functional theory in order to compare the insertion process for these three isovalent molecules. The relative stabilities of the adduct and insertion forms are calculated. The reaction barrier between these two forms are estimated for each system from the $^4A''$ and $^4A'$ potential energy curves defined in terms of the C−X (X=O,S) intrinsic reaction coordinate. The barrier to metal insertion from the side-on structure is rather low (ca 4 kcal/mol) for CO_2 and CS_2, however, whereas V(CO_2) is well above the OVCO insertion product, the V(CS_2) complex is only 4.2 less stable than SVCS. Consequently, coordination of CS_2 to metal centers is stronger than that of CO_2. Our calculations indicate no energy barrier for the insertion of V in the CS bond of OCS, whereas the insertion in the CO bond is less favored than in CO_2. We show that each insertion reaction proceeds on a single potential energy surface. Differences in the energetics of the three reactions are related to the molecular properties of CO_2, CS_2, and OCS.

1. Introduction

Carbon dioxide (CO_2), carbon disulfide (CS_2), and carbonyl sulfide (OCS) are isovalent linear triatomic molecules. Their reactions with metal centers are in the focus in various research areas of chemistry and material science. The catalytic conversion of CO_2 into other carbon compounds is receiving a continuous attention,[1−3] whereas CS_2 and OCS have recently been considered as possible sulfur sources for preparing thin layers of semiconductor materials.[4]

Despite their structural similarities, these closely related molecules show very different reactions with transition metals.[5,6] CS_2 is generally very reactive toward metal centers: it forms coordination complexes with almost every transition metal and it undergoes a variety of insertion and disproportionation reactions. The CO_2 molecule is more reluctant in these reactions, and the CO_2 complexes (if they exist at all) are always less stable than the corresponding CS_2 complexes. The cleavage of the C−O and C−S bonds in organometallic reactions of CO_2 and CS_2 is rare, whereas in contrast, the abstraction of sulfur from OCS is quite common.

Our recent density functional study on the Ti + CO_2 system[7] indicated that the ground state Ti atom inserts spontaneously into CO_2; that is, no activation barrier exists between the separated reactants (Ti(s^2d^2) + CO_2) and the OTiCO insertion product. We showed that the reaction is initiated by metal−CO_2 electron transfer and proceeds via the formation of a η^2_{CO} (side-on) Ti(CO_2) adduct, which, however, does not represent an energy minimum with respect to the reaction coordinate because the system follows a downhill path towards OTiCO. The insertion product was shown to be 25 kcal/mol more stable than the η^2_{CO} structure, and it was described as a carbonyl complex, where the CO ligand is relatively weakly bound to TiO.

In the present work, we investigate the insertion reaction of the V(s^2d^3) atom with CO_2, CS_2, and OCS. Our main goal is to compare the insertion process for the three isovalent ligands. We determine the relative stability of the adduct and insertion forms of the V + CO_2, V + CS_2, and V + OCS systems, and we estimate the reaction barriers between the two forms. Differences in the energetics of the three reactions will be pointed out, and they will be related to the molecular properties of the CO_2, CS_2, and OCS reactants.

2. Computational Details

Our strategy in exploring the reaction path of the metal insertion is similar to that reported in ref 7 in that we map the ground-state potential energy surfaces between the region of complex formation and the insertion product by defining an intrinsic reaction coordinate. However, instead of performing a steepest descent geometry optimization toward the global minimum,[7] in the present work, we carried out geometry optimizations for a set of fixed C−O (or C−S) bond lengths. Thus the reaction coordinate of the metal insertion is defined as the C−O (C−S) separation of the cleaved bond. The C−O (C−S) separation was varied from the values corresponding to the free ligands to those calculated in the insertion products. As a result of this procedure, we obtain potential energy curves on which the η^2_{CO} and η^2_{CS} complexes, the insertion products, and the corresponding transition structures can easily be located. Normal coordinate analysis carried out for the stationary points revealed that the imaginary frequency of the transition structures basically correspond to the C−O (C−S) stretching motion.

* To whom correspondence should be addressed.

10.1021/jp014034k CCC: $22.00
Published on Web 03/26/2002

TABLE 1: Calculated and Experimental Properties for the Ground States of CO_2, CS_2, and OCS[a]

	CO_2		CS_2		OCS	
	calcd	expt	calcd	expt	calcd	expt
E	−188.6506		−834.5576		−511.6056	
R(CO)	1.160	1.162[b]			1.156	1.156[d]
R(CS)			1.558	1.556[c]	1.568	1.561[d]
$\omega(\sigma)$	2401	2349[e]	1532	1535[e]	2101	2072[d]
$\omega(\sigma)$	1365	1333	668	658	868	866
$\omega(\pi)$	676	667	398	397	523	520
EA_{ad}	−0.30	-0.6 ± 0.2[f]	0.54	1.0 ± 0.2[f]	0.19	0.46 ± 0.2[f]
D_0(C−O)[g]	126.7	125.7[h]			162.8	158.2[h]
D_0(C−S)[g]			105.4	104.0[h]	74.6	71.5[h]

[a] Units: total energies (E) in hartree, bond lengths (R) in Å, vibrational frequencies (ω) in cm^{-1}, adiabatic electron affinities (EA_{ad}) in eV, bond dissociation energies (D_0) in kcal/mol. [b] From ref 17. [c] From ref 18. [d] From ref 19. [e] From ref 20. [f] From ref 21. [g] Calculated as the ZPE corrected energies of the $XCY(^1\Sigma^+) \rightarrow X(^3P) + CY(^1\Sigma^+)$ reactions (X,Y = O,S). [h] From atomization energies listed in JANAF tables (see ref 22).

The energy values on the investigated potential energy surfaces will always be given with respect to the separated ground-state species ($V(s^2d^3) + CO_2(^1\Sigma_g)$, etc.). The single determinant we have chosen here to describe the ground state ($^4F(s^2d^3)$) of V is the one that yields the lowest energy ($E = -943.9048$ hartree) of all possible pure ^4F state determinants. The occupation of the spin−orbitals corresponding to this determinant is $(4s)^2\ (3d_0^{\alpha})^1\ (3d_1^{\alpha})^1\ (3d_2^{\alpha})^1$.

The energy calculations and the geometry optimizations were carried out at the B3LYP level[8−10] of density functional theory. The basis sets we used include the (14,9,5)/(8,5,3) all-electron basis set from Schäfer et al.[11] supplemented with two p functions[12] and a diffuse d function[13] for the V atom and the 6-311 + G(2d) basis set[14] for C, O, and S. The stability of the wave function for symmetry breaking has been checked for each identified stationary point. All calculations were performed with the Gaussian94 program.[15]

We mention that by applying the present methodology to the Ti + CO_2 system we obtained very similar results to those presented in ref 7. Namely, only an extremely small (0.5 kcal/mol) energy barrier is predicted toward the OTiCO product and the η^2_{CO} Ti(CO_2) structure lies 23 kcal/mol above OTiCO.

3. Results and Discussion

3.1. Molecular Properties of CO_2, CS_2, and OCS. First, we present our results obtained for the free CO_2, CS_2, and OCS molecules. Some selected molecular properties of the three molecules calculated at the B3LYP/6-311 + G(2d) level are compared with experimental data in Table 1. As expected, the experimental geometries and the observed vibrational frequencies are well reproduced at this level of theory. The accuracy of the B3LYP/6-311 + G(2d) calculations for these properties is comparable to that of the CCSD(T)/6-311+ G(3df) method.[16]

In addition to structural and vibrational properties, two sets of energetical data are listed in Table 1. The adiabatic electron affinities, which indicate the ability of the molecules to bind an electron (and therefore they are closely related to the strength of the metal−ligand interaction), were calculated as $EA_{ad}(L) = E_{tot}(L) - E_{tot}(L^-) + \Delta ZPE$, where $E_{tot}(L)$ and $E_{tot}(L^-)$ denote the total energies of the neutral and ionic forms of geometry optimized L = CO_2, CS_2, and OCS molecules, whereas ΔZPE is the zero-point vibrational energy correction evaluated from the calculated harmonic frequencies. The ZPE corrected C−O and C−S bond dissociation energies (D_0(C−O) and D_0(C−S)), which will be associated with the energetics of the insertion reactions, are also given in Table 1.

The comparison of the calculated EA_{ad} values with the experimental data shows that, although the discrepancies are quite considerable (they range between 0.3 and 0.4 eV), the present method reproduces the trend in the measured data for the CO_2−OCS−CS_2 series. On the other hand, the experimental bond dissociation energies are accurately reproduced at the B3LYP/6-311 + G(2d) level.

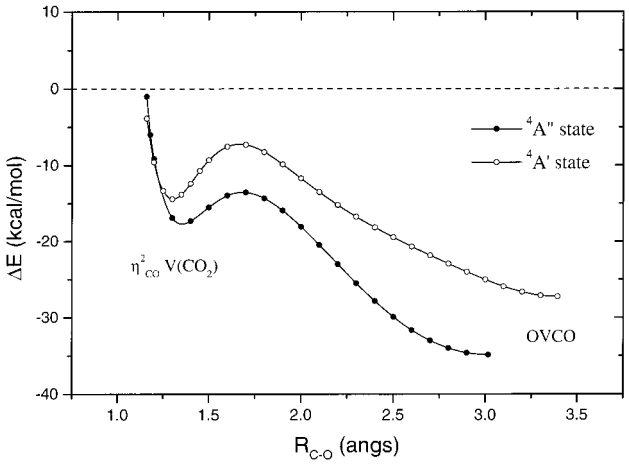

Figure 1. $^4A''$ and $^4A'$ potential energy curves for the V + CO_2 → OVCO insertion reaction. Energies are given with respect to separated $V(s^2d^3) + CO_2$.

3.2. Insertion into CO_2. Because here we are concerned with the minimum energy path of the insertion reactions, we assume coplanar arrangement of the interacting fragments along the entire reactions. For $V(s^2d^3) + CO_2$, we considered both quartet states ($^4A''$ and $^4A'$) derived within the C_s symmetry, which are associated with the $(a'')^1(a')^1(a')^1$ and $(a'')^1(a')^1(a'')^1$ configurations of the unpaired electrons, respectively. The variation of the total electronic energy as a function of the R_{C-O} reaction coordinate of the V + CO_2 → OVCO insertion is depicted in Figure 1 for both states.

The inserted OVCO molecule represents the global energy minimum for both surfaces. The ground state of the OVCO molecule is $^4A''$, which lies 34.9 kcal/mol below the $V(s^2d^3) + CO_2$ level, and it is 7.6 kcal/mol more stable than the $^4A'$ state. The side-on coordinated V(CO_2) complex is predicted to be a local minimum on both surfaces, but it lies much higher in energy than the insertion product (17.2 and 12.8 kcal/mol above OVCO on $^4A''$ and $^4A'$ surfaces, respectively). The barrier to metal insertion from the η^2_{CO} structure is rather low (4.1 and 7.2 kcal/mol on the $^4A''$ and $^4A'$ surfaces); therefore, it is quite likely that similarly to Ti the ground-state V atom inserts into CO_2 spontaneously to yield OVCO. These results are consistent with the findings of matrix isolation experiments[23,24] in that neither thermally evaporated[23] nor laser ablated[24] V atoms gave coordinated 1:1 complexes with CO_2, but in both cases, only insertion products were detected.

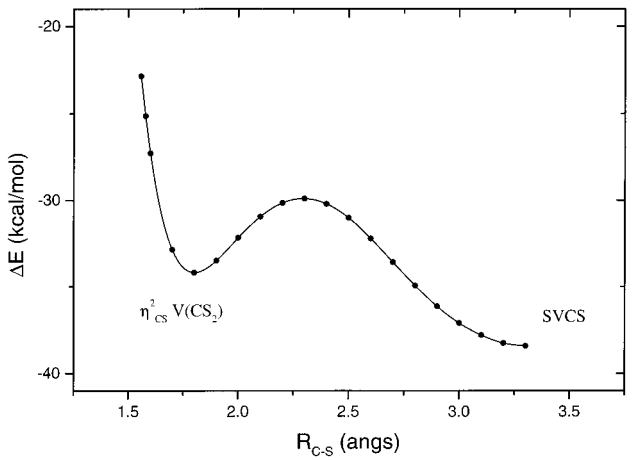

Figure 2. $^4A''$ potential energy curve for the V + CS_2 → SVCS reaction.

The OVCO molecule has only been isolated by the laser-ablation technique, because, in the former study, the OVCO species has shown to react with an additional CO_2 leading to the formation of the OV(CO)(CO_2) complex. The matrix isolated OVCO, however, does not seem to be in the $^4A''$ electronic state. Although previous BP86 calculations[24] predicted the $^2A'$ state of OVCO 9 kcal/mol above the most stable $^4A''$ state, the observed CO stretching frequency (1881 cm^{-1}) and the corresponding isotopic shifts were more consistent with the $^2A'$ state. Our B3LYP calculations also predict the $^2A'$ state clearly above the $^4A''$ state; however, we point out that there are a few indications that the present level of DFT might not provide reliable energetics for the doublet states of OVCO. For instance, wave function stability tests revealed a symmetry breaking problem[25] for the $^2A'$ and $^2A''$ states; that is, we found that the symmetry-broken solutions for these states became lower in energy than the C_s solutions. In addition, it appears that both $^2A'$ and $^2A''$ states of OVCO are seriously spin contaminated, indicating that a multiconfigurational approach is likely to be applied for correct description of the doublet states. Clearly, systematic high level ab initio study is required to check if the quartet and doublet state surfaces cross in the OVCO region.

3.3. Insertion into CS_2. The minimum energy path connecting the η^2_{CS} V(CS_2) and SVCS structures on the $^4A''$ surface is shown in Figure 2. For all our investigated systems, we found the $^4A'$ curves always above $^4A''$; therefore, for the remaining insertion reactions, we show only the ground state ($^4A''$) curves. The exothermicity of the V + CS_2 → SVCS insertion (38.5 kcal/mol) is quite similar to that of V + CO_2 → OVCO (34.9 kcal/mol); however, there is a striking difference between the CS_2 and CO_2 potential energy curves. Although the side-on complex of V(CO_2) is well above the insertion product (see Figure 1), the η^2_{CS} V(CS_2) complex is only 4.2 kcal/mol less stable than SVCS. The energy barrier from the side-on complex to the inserted molecule is 4.3 kcal/mol.

The enhanced stability of the V(CS_2) complex as compared to V(CO_2) can be related to the difference between the electron affinities of the two ligands. The adiabatic electron affinities of the CO_2 and CS_2 ligands (see Table 1) suggest that the metal → ligand π back donation, which is identified as the main component of the metal−ligand bonding interaction in these types of complexes,[26] is energetically more favorable for CS_2. These results thus nicely reflect the general trend that shows that the coordination of CS_2 to metal centers is always stronger than that of CO_2.[5,6]

TABLE 2: B3LYP Predicted Equilibrium Properties of the OVCO Insertion Product, η^2_{CO} V(CO_2), and the Corresponding Transition Structure ($^4A''$)[a]

	OVCO	V(CO_2)	TS
E	−1132.6110	−1132.5835	−1132.5771
R(V−O)	1.611	1.852	1.744
R(V−C)	2.058	2.020	2.009
R(C−O)	1.138	1.189/1.356	1.159/1.681
α(OVC)	110.0	40.7	52.7
α(VCO)	165.6	166.3	177.9
α(OCO)		130.8	122.4
ω_1(a′)	2067 (1616)	1810 (787)	1962 (790)
ω_2	981 (270)	914 (199)	843 (177)
ω_3	376 (23)	714 (74)	530 (1)
ω_4	319 (3)	456 (2)	341 (3)
ω_5	124 (17)	311 (12)	394i (298)
ω_6(a″)	286 (2)	395 (0)	322 (0)
μ	4.41	7.30	6.31

[a] Units: total energies (*E*) in hartree; bond lengths (*R*) in Å, vibrational frequencies (ω_e) in cm^{-1}, IR intensities (in parentheses) in km/mol, dipole moment (μ) in Debye.

TABLE 3: B3LYP Predicted Equilibrium Properties of the SVCS Insertion Product, η^2_{CS} V(CS_2), and the Corresponding Transition Structure ($^4A''$)[a]

	SVCS	V(CS_2)	TS
E	−1778.5237	−1778.5169	−1778.5107
R(C−S)	1.546	1.800/1.613	2.293/1.566
R(V−C)	1.960	1.987	1.955
R(V−S)	2.072	2.235	2.144
α(SCS)		133.4	126.4
α(SVC)	110.4	50.0	67.9
α(VCS)	171.4	154.5	173.6
ω_1(a′)	1278 (791)	1117 (426)	1219 (609)
ω_2	544 (77)	544 (39)	496 (55)
ω_3	371 (10)	438 (13)	366 (1)
ω_4	260 (3)	324 (19)	240 (5)
ω_5	73 (7)	191 (8)	204i (108)
ω_6(a″)	231 (14)	281 (5)	257 (7)
μ	5.11	6.83	5.29

[a] Units: same as in Table 2.

Although the reactions of carbon dioxide with transition metals have been studied extensively in matrix isolation IR studies,[23,24,27,28−31] those of CS_2 have only been investigated for a few first-row transition metals.[32,33] Matrix reactions of Ni with CS_2 have been shown to give Ni(CS_2)$_n$ (n = 1−3) complexes,[32] whereas in a recent matrix isolation/DFT report,[33] the formation of M(CS_2) and SMCS species has been observed for M = Co, Ni, and Cu. One expects from the present results that the formation of both types of complexes is feasible in the V + CS_2 reaction. The predicted structural and vibrational parameters of the $^4A''$ states of the η^2_{CS} form of V(CS_2) and the SVCS molecule, which are listed in Table 3, may serve as a starting point in identifying these species. We have also considered the doublet states of both molecules which are calculated higher in energy than the corresponding quartet species. However, as in the case of OVCO, the doublet states of SVCS are highly spin contaminated, and we encounter wave function instabilities for these states.

We also note that the reactivity of the V^+ cation and CS_2 has recently been examined in the gas phase using guided ion beam mass spectrometry and DFT.[34] Although the nature of the metal−ligand bond and the driving forces in the V + CS_2 → SVCS and V^+ + CS_2 → $SVCS^+$ reactions might be quite different, it is interesting to compare the relative energies of the analogue species of the two reactions. The comparison of the $^4A''$ potential energy curve shown in Figure 2 with that

TABLE 4: Predicted Ground State Properties of the SVCO, OVCS, and η^2_{CO} V(OCS) and the Transition Structure (TS) Connecting the OVCS and V(OCS) Species[a]

	SVCO	OVCS	V(OCS)	TS
E	−1455.5921	−1455.5447	−1455.5371	−1455.5062
R(V−X)	2.077	1.607	1.877	1.708
R(V−C)	2.034	1.983	2.012	1.975
R(C−Y)	1.137	1.548	1.308/1.619[b]	1.886/1.560[b]
α(XVC)	106.4	111.5	39.2	61.1
α(VCY)	170.8	164.9	161.1	174.7
α(OCS)	−	−	134.2	122.3
ω_1 (a′)	2082 (1274)	1273 (816)	1313 (348)	1242 (652)
ω_2 (a′)	538 (58)	992 (284)	894 (364)	838 (231)
ω_3 (a′)	380 (32)	374 (0)	606 (30)	358 (4)
ω_4 (a′)	316 (1)	288 (4)	422 (11)	280 (14)
ω_5 (a′)	77 (6)	103 (12)	218 (21)	420i (404)
ω_6 (a″)	293 (0)	217 (13)	317 (7)	228 (7)
μ	5.50	4.13	7.15	4.63

[a] Units: same as in Table 2 [b] *R*(C−O)/*R*(C−S) bond lengths.

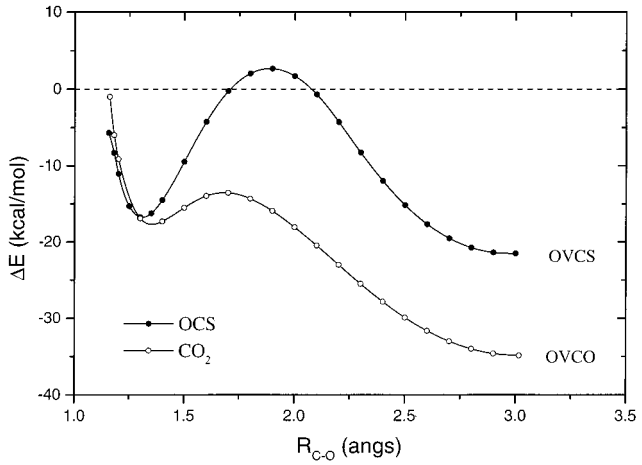

Figure 3. ^{4}A″ potential energy curves for the V + OCS → OVCS and V + CO_2 → OVCO reactions.

obtained at the B3LYP/6-311 + G* level for the analogue ^{3}A″ state of V^+ + CS_2 (see Figure 5 in ref 34) reveals a close resemblance in that, in both cases, the 1:1 complex and the insertion product have similar stabilities, and they are separated by a low energy barrier.

3.4. Insertion into OCS. In principle, the reaction of OCS with atomic vanadium can follow two distinct channels corresponding to the formation of the OVCS and SVCO insertion products. The ^{4}A″ potential energy curves for these two routes are shown in Figures 3 and 4. In these figures, we also depicted the ^{4}A″ curves of the V + CO_2 (Figure 3) and V + CS_2 (Figure 4) systems, so as the activation of the C−O and C−S bonds in OCS can be paralleled with those in CO_2 and CS_2.

As Figure 3 indicates, the V + OCS → OVCS process is exothermic, but the stability of the OVCS molecule relative to reactants (21.5 kcal/mol) is decreased as compared to OVCO (34.9 kcal/mol). The stabilities of the η^2_{CO} V(OCS) and η^2_{CO}

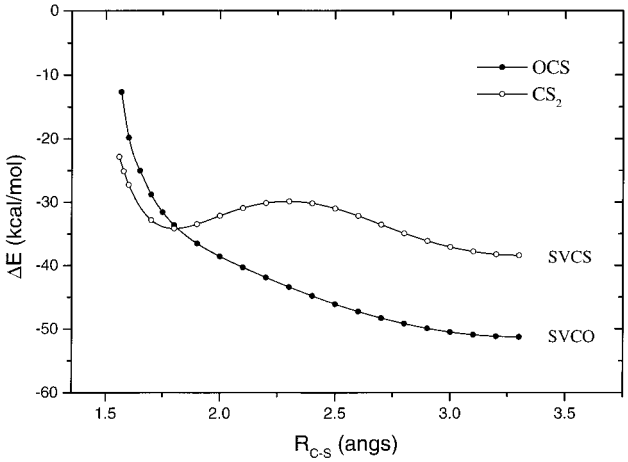

Figure 4. ^{4}A″ potential energy curves for the V + OCS → SVCO and V + CS_2 → SVCS reactions.

V(CO_2) complexes are about the same (16.8 and 17.7 kcal/mol, respectively), but in contrast to V + CO_2, there is a considerable energy barrier (19.4 kcal/mol) on the V + OCS surface to reach the OVCS insertion product. On the other hand, the metal insertion into the C−S bond of OCS has no energy barrier at all (see Figure 4) because the total energy of the system decreases monotonically when going from the hypothetical η^2_{CS} V(OCS) structure toward the insertion product. The SVCO molecule is the most stable species among the investigated structures; it is stabilized by 51.3 kcal/mol with respect to V + OCS.

These results show quite clearly that it is much easier to cleave the C−S bond in OCS than in CS_2, whereas the activation of the C−O bond is energetically less favored in OCS than in CO_2. A comparison of the bond dissociation energies of the three ligands offers a reasonable explanation for this finding. It appears from the D_0(C−O) and D_0(C−S) values (Table 1) that in OCS the C−S bond is weakened and the C−O bond is strengthened relative to those in the CS_2 and CO_2 molecules. Therefore, it is not surprising that the chemistry of the transition-metal−OCS complexes is dominated by reactions that involve cleavage of the C−S bond.[5]

On the basis of the predicted stability data, one expects the SVCO species to be the most feasible product formed in the V + OCS reaction; however, the metastable η^2_{CO} V(OCS) and OVCS molecules might also be produced via other reaction channels (photolysis, VO + CS, etc.). Our recent matrix isolation experiments for the V + OCS system indicate that indeed vanadium inserts spontaneously into the C−S bond, but we found no spectroscopic evidence for the formation of the two metastable species. A detailed analysis of the matrix isolation IR spectra and DFT results will be reported elsewhere,[35] but here we present only the predicted ground state (^{4}A″) properties of SVCO, OVCS, V(OCS), and the CO insertion transition structure (Table 4). The calculated vibrational frequencies

TABLE 5: Calculated and Experimental Equilibrium Properties of VO, VS, CO, and CS[a]

	VO ($^4\Sigma^-$)		VS ($^4\Sigma^-$)		CO		CS	
	calcd	expt[b]	calcd	expt	calcd	expt[b]	calcd	expt[b]
E	−1019.2332		−1342.2032		−113.3520		−436.2527	
R_e	1.589	1.59	2.068	−	1.126	1.128	1.535	1.534
ω_e	1037	1011	538	580[c]	2211	2170	1296	1285
D_0	148.1	148.6[d]	102.9	106.6[d]	250.7	256.2[d]	162.6	169.4[d]

[a] Units: total energies (*E*) in hartree, bond lengths (R_e) in Å, vibrational frequencies (ω_e) in cm^{-1}, ZPE corrected bond dissociation energies (D_0) in kcal/mol. [b] Experimental data are taken from ref 36 unless noted otherwise. [c] From ref 37. [d] From ref 22.

indicate that the three minima could be easily distinguished relying upon the observed IR absorptions. As we did for the OVCO and SVCS molecules, we examined the doublet states of the SVCO and OVCS insertion products as well. The doublet states are calculated to be higher in energy than the corresponding quartet states but these states are again highly spin contaminated.

3.5. Overall Energetics. We saw in the previous sections that the stability of the XVCY insertion products (X,Y = O,S) relative to the V + XCY asymptotes varies in the 21−51 kcal/mol energy range and the order of increasing stability is OVCS (21.5) < OVCO (34.9) < SVCS (38.5) < SVCO (51.3 kcal/mol). Because the insertion species are characterized as XV−CY complexes, it is interesting to determine their XV−CY binding energies as well. For this purpose, we have calculated the ground state properties of the VX and CY diatomic molecules. The results are compiled in Table 5 along with the available experimental data. It is seen that the present level of theory provides quite reasonable spectroscopic and thermochemical data not only for the CY (and XCY) molecules but also for the transition metal VX species. The spectroscopic parameters obtained at the present level of theory for $VO(^4\Sigma^-)$ and $VS(^4\Sigma^-)$ are very similar to those from CCSD(T) calculations.[38]

The calculated XV−CY binding energies (i.e., the enthalpies of the XV−CY → VX + CY reactions) are 16.2 (OVCO), 23.2 (SVCO), 36.9 (OVCS), and 42.6 kcal/mol (SVCS), indicating that they do not follow the same sequence as shown above. As a general trend, one observes that the XV−CO bonds are about 20 kcal/mol less stable than the corresponding XV−CS bonds, whereas the CO and CS molecules form 6−7 kcal/mol stronger bonds with VS than with VO. Despite the large differences in the energetics, the equilibrium structure of these products is very similar in that they all have α(XVC) and α(VCY) angles that are close to 110° and 170°, respectively (see Tables 2-4). We may also observe that the V−C bond lengths correlate well with the trend obtained for the XV−CY binding energies.

From the energies of the V + XCY → XVCY and XVCY → VX + CY reactions, we can now estimate the energetics of the V + XCY → VX + CY abstraction reactions, which are −18.7, +4.1, +15.4, and −28.1 kcal/mol for the OVCO, SVCS, OVCS, and SVCO products, respectively. Here, the negative (positive) sign refers to exothermic (endothermic) V + XCY → VX + CY reaction. The corresponding ZPE corrected values (in the same order) are −21.4, +2.5, +13.8, and −29.2 kcal/mol. Note that the same values are obtained from the energies of the XCY → CY + X and V + X → VX reactions, i.e., simply from the D_0(C−X) and D_0(V−X) values listed in Tables 1 and 5. The calculated abstraction energies can thus be compared to experimental data, which are −22.9 (VO + CO), −2.6 (VS + CS), +9.6 (VO + CS), and −35.1 (VS + CO) kcal/mol. We see that our calculations always underestimate the stability of the VX + CY products relative to V + XCY. The discrepancies, which we think originate mostly from the inaccurate description of the V atom at the present level of theory, are not significant; they range between 2 and 6 kcal/mol.

The decomposition of the abstraction energies into the XCY → CY + X and V + X → VX terms offers a simple interpretation for the trend obtained in the energetics. For instance, the V + CO_2 → VO + CO reaction is exothermic (by −21.4 kcal/mol) because the energy required to cleave the C−O bond in carbon dioxide (126.7 kcal/mol) is compensated, and even exceeded, by the energy gained in the VO formation (−148.1 kcal/mol). In fact, the driving force of the V + CO_2 → OVCO insertion reaction is the formation of the strong metal−oxide bond. Because the C−O bond dissociation energy in OCS (162.8 kcal/mol) is much higher than in CO_2, the V + OCS → VO + CS reaction becomes endothermic. Although the VS molecule is about 45 kcal/mol less stable than VO, the C−S bond in OCS is so weak (D_0(C−S) = 74.6 kcal/mol) that V + OCS → VS + CO is the most favored abstraction reaction. On the other hand, the stability of the C−S bond in CS_2 (105.4 kcal/mol) is close to that of the VS molecule (102.9 kcal/mol); therefore, the energy of the VS + CS products is very similar to the V + CS_2 reactants.

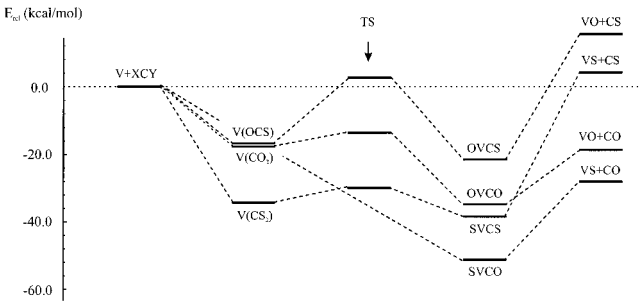

Figure 5. Overall energetics of the V + XCY → VX + CY (X,Y = O,S) reactions (based on the ZPE uncorrected energies).

The overall energetics of the $V(s^2d^3)$ + $XCY(^1\Sigma^+)$ → $VX(^4\Sigma^-)$ + $CY(^1\Sigma^+)$ reactions is summarized in Figure 5. As noted before, the ground state of the V(XCY) association complexes and the XVCY insertion products is $^4A''$. Moreover, the $VX(^4\Sigma^-)$ + $CY(^1\Sigma^+)$ products correlate with the $^4A''$ state of the corresponding XVCY molecules, which means that once the V(XCY) ($^4A''$) association complexes are formed from V + XCY the entire V(XCY) → TS → XVCY → VX + CY reaction proceeds on a single potential energy surface. This might not be true generally, however, for M + XCY type reactions of other transition metal atoms, because surface crossings between different states may occur on the way from M(XCY) to MX + CY. Surface crossings may also be present in the V + XCY entrance channel of the reactions, where surfaces derived from close-lying metal atomic states may intersect and may give rise to an appreciable energy barrier. The evaluation of accurate potential energy surfaces in this region (i.e., large and intermediate M−XCY separations) is a great challenge for present day quantum chemistry, and one should definitely go beyond the methodology applied in the present work.

4. Concluding Remarks

We have shown, by means of a B3LYP DFT study, that ground-state vanadium atoms undergo a spontaneous insertion reaction in the CS bond of OCS molecules. This result is in line with our recent matrix isolation experiments.[35]

The comparative study of the $V(s^2d^3)$ + XCY → V(XCY) → TS → XVCY → VX + CY reactions with XCY = CO_2, CS_2, and OCS shows that, from the coordination complex to the insertion product, they all proceed on a single potential energy surface ($^4A''$) along one intrinsic reaction coordinate, the CX (X = O,S) bond length.

Comparison of relative energies show that insertion products are always more stable than the related coordination species, with the following increasing orders of stability: V(OCS) < $V(CO_2)$ ≪ $V(CS_2)$ and OVCS < OVCO < SVCS ≪ SVCO. Only V + CO_2 → VO + CO and V + OCS → VS + CO are exothermic, with a low or no insertion reaction energy barrier.

Further work is in progress on the comparative theoretical study of reactions of first row transition metal atoms with the OCS molecule.

Acknowledgment. This work is part of the European COST Chemistry D9 Action (COST D9/0012/98) and a Hungarian-French intergovernmental research program (Tét, F-5/1999; Balaton 2000/00851QL). I.P. acknowledges the financial support from the Hungarian Research Foundation (OTKA, Grant No. T029926) and the Bolyai Fellowship. J.M. acknowledges the allocation of computer time (IDRIS Project No. 11441).

References and Notes

(1) Braunstein, P.; Matt, D.; Nobel, D. *Chem. Rev.* **1988**, *88*, 747.
(2) Gibson, D. H. *Chem. Rev.* **1996**, *96*, 2063.
(3) Yin, X.; Moss, J. R. *Coord. Chem. Rev.* **1999**, *181*, 27.
(4) Almond, M.; Cockayne, B.; Cooke, S. A.; Rice, D. A.; Smith, P. C.; Wright, P. J. *J. Mater. Chem.* **1996**, *6*, 1639.
(5) Ibers, J. A. *Chem. Soc. Rev.* **1982**, *11*, 57.
(6) Pandey, K. K. *Coord. Chem. Rev.* **1995**, *140*, 37.
(7) Pápai, I.; Mascetti, J.; Fournier, R. *J. Phys. Chem. A* **1997**, *101*, 4465.
(8) Becke, A. D. *J. Chem. Phys.* **1993**, *98*, 5648.
(9) Lee, C.; Yang, W.; Parr, R. G. *Phys. Rev. B* **1988**, *37*, 785.
(10) Stephens, P. J.; Devlin, F. J.; Chabalowski, C. F.; Frisch, M. J. *J. Phys. Chem.* **1994**, *98*, 11623.
(11) Schäfer, A.; Horn, H.; Ahlrichs, R. *J. Chem. Phys.* **1992**, *37*, 2571.
(12) Wachters, A. J. H. *J. Chem. Phys.* **1970**, *52*, 1033.
(13) Hay, P. J. *J. Chem. Phys.* **1977**, *66*, 4377.
(14) Krishnan, R.; Binkley, J. S.; Seeger, R.; Pople, J. A. *J. Chem. Phys.* **1980**, *72*, 650. Frisch, M. J.; Pople, J. A.; Binkley, J. S. *J. Chem. Phys.* **1984**, *80*, 3265.
(15) Frisch, M. J.; Trucks, G. W.; Schlegel, H. B.; Gill, P. M. W.; Johnson, B. G.; Robb, M. A.; Cheeseman, J. R.; Keith, T.; Petersson, G. A.; Montgomery, J. A.; Raghavachari, K.; Al-Laham, M. A.; Zakrzewski, V. G.; Ortiz, J. V.; Foresman, J. B.; Peng, C. Y.; Ayala, P. Y.; Chen, W.; Wong, M. W.; Andres, J. L.; Replogle, E. S.; Gomperts, R.; Martin, R. L.; Fox, D. J.; Binkley, J. S.; Defrees, D. J.; Baker, J.; Stewart, J. P.; Head-Gordon, M.; Gonzalez, C.; Pople, J. A. *Gaussian 94*, Revision E.3, Gaussian, Inc., Pittsburgh, PA, 1995.
(16) Gutsev, G. L.; Bartlett, R. J.; Compton, R. N. *J. Chem. Phys.* **1998**, *108*, 6756.
(17) Herzberg, G. *Molecular Spectra and Molecular Structure III. Electronic Spectra and Electronic Structure of Polyatomic Molecules*; Van Nostrand Reinhold: New York, 1966.
(18) Suzuki, I. *Bull. Chem. Soc. Jpn.* **1975**, *48*, 1685.
(19) Lahaye, J.-G.; Vandenhaute, R.; Fayt, A. *J. Mol. Spectrosc.* **1987**, *123*, 48.
(20) *CRC Handbook of Chemistry and Physics*; Lide, D. R., Ed.; CRC Press: Boca Raton, FL, 1994.
(21) Compton, R. N.; Reinhardt, P. W.; Cooper, C. D. *J. Chem. Phys.* **1975**, *63*, 3821.
(22) Chase, M. W., Jr.; Davies, A. C.; Downey, J. R., Jr., Fruirip, D. J.; McDonald, R. A.; Syverud, A. N. JANAF Tables, *J. Phys. Chem. Ref. Data* **1985,** *11*, Suppl. 1.
(23) Mascetti, J.; Tranquille, M. *J. Phys. Chem.* **1988**, *92*, 2177.
(24) Zhou, M.; Andrews, L. *J. Phys. Chem. A* **1999**, *103*, 2066.
(25) Sherrill, C. D.; Lee, M. S.; Head-Gordon, M. *Chem. Phys. Lett.* **1999**, *302*, 425.
(26) Rosi, M.; Sgamellotti, A.; Tarantelli, F.; Floriani, C. *J. Organomet. Chem.* **1987**, *332*, 153.
(27) Galan, F.; Fouassier, M.; Tranquille, M.; Mascetti, J.; Pápai, I. *J. Phys. Chem.* **1997**, *101*, 2626.
(28) Souter, P. F.; Andrews, L. *J. Am. Chem. Soc.* **1997**, *119*, 7350.
(29) Zhou, M.; Andrews, L. *J. Am. Chem. Soc.* **1998**, *120*, 13230.
(30) Zhou, M.; Liang, B.; Andrews, L. *J. Phys. Chem. A* **1999**, *103*, 2013.
(31) Zhang, L. N.; Wang, X. F.; Chen, M. H.; Qin, Q. Z. *Chem. Phys.* **2000**, *254*, 231.
(32) Huber, H.; Ozin, G. A.; Power, W. J. *Inorg. Chem.* **1977**, *16*, 2234.
(33) Zhou, M.; Andrews, L. *J. Phys. Chem. A* **2000**, *104*, 4394.
(34) Rue, C.; Armentrout, P. B.; Kretzschmar, I.; Schroder, D.; Harvey, J. N.; Schwarz, H. *J. Chem. Phys.* **1999**, *110*, 7858.
(35) Gwizdala, S.; Redman, H.; Almond, M. J.; Pápai, I.; Mascetti, J. to be published.
(36) Huber, K. P.; Herzberg, G. *Constants of diatomic molecules*; Van Nostrand Reinhold: New York, 1979.
(37) DeVore, T. C.; Franzen, H. F. *High Temp. Sci.* **1975**, *7*, 220.
(38) Bauschlicher, C. W., Jr.; Maître, P. *Theor. Chim. Acta* **1995**, *90*, 189.